Monthly Notices
of the
ROYAL ASTRONOMICAL SOCIETY

MNRAS **430,** 1008–1017 (2013) doi:10.1093/mnras/sts671

Infrared observations of the candidate double neutron star system PSR J1811−1736

R. P. Mignani,[1,2]★ A. Corongiu,[3] C. Pallanca[4] and F. R. Ferraro[4]

[1]*Mullard Space Science Laboratory, University College London, Holmbury St Mary, Dorking, RH5 6NT*
[2]*Kepler Institute of Astronomy, University of Zielona Góra, Lubuska 2, 65-265, Zielona Góra, Poland*
[3]*INAF Osservatorio Astronomico di Cagliari, Località Poggio dei Pini, Strada 54, I-09012 Capoterra, Italy*
[4]*Dipartimento di Fisica e Astronomia, Università degli Studi di Bologna, via Ranzani 1, I-40127 Bologna, Italy*

Accepted 2012 December 19. Received 2012 December 19; in original form 2012 September 15

ABSTRACT

PSR J1811−1736 (P_s = 104 ms) is an old (∼1.89 Gyr) binary pulsar (P_{orb} = 18.8 d) in a highly eccentric orbit (e = 0.828) with an unidentified companion. Interestingly, the pulsar timing solution yields an estimated companion mass of $0.93\,M_\odot \leq M_C \leq 1.5\,M_\odot$, compatible with that of a neutron star. As such, it is possible that PSR J1811−1736 is a double neutron star (DNS) system, one of the very few discovered so far. This scenario can be investigated through deep optical/infrared (IR) observations. We used *J*- *H*- and *K*-band images, obtained as part of the UK Infrared Telescope (UKIRT) Infrared Deep Sky Survey (UKIDSS), and available in the recent Data Release 9 Plus, to search for the undetected companion of the PSR J1811−1736 binary pulsar. We detected a possible companion star to PSR J1811−1736 within the 3σ radio position uncertainty (1.32 arcsec), with magnitudes $J = 18.61 \pm 0.07$, $H = 16.65 \pm 0.03$ and $K = 15.46 \pm 0.02$. The star colours are consistent with either a main sequence (MS) star close to the turn-off or a lower red giant branch (RGB) star, at a pulsar distance of ∼5.5 kpc and with a reddening of $E(B-V) \sim 4.9$. The star mass and radius would be compatible with the constraints on the masses and orbital inclination of the binary system inferred from the mass function and with the lack of radio eclipses near superior conjunction. Thus, it is possible that it is the companion to PSR J1811−1736. However, based on the star density in the field, we estimated quite a large chance coincidence probability of ∼0.27 between the pulsar and the star, which makes the association unlikely. No other star is detected within the 3σ pulsar radio position down to $J \sim 20.5$, $H \sim 19.4$ and $K \sim 18.6$, which allows us to rule out a MS companion star earlier than a mid-to-late M spectral type.

Key words: stars: neutron – pulsars: individual: PSR J1811–1736.

1 INTRODUCTION

The radio pulsar PSR J1811−1736 (P_s = 104 ms) was detected at 1374 MHz (Lyne et al. 2000) during the Parkes Multibeam Pulsar Survey (Manchester, Lyne & Camilo 2001). It is in a binary system, with an orbital period P_{orb} = 18.8 d and a high eccentricity e = 0.828 (Corongiu et al. 2007). The updated timing parameters, including general relativistic effects, give a period derivative $\dot{P}_s \approx 9.01(5) \times 10^{-19}$ s s^{-1}, which yields a spin-down age $\tau_{SD} \approx 1.89 \times 10^9$ yr and a surface magnetic field $B_{surf} \approx 9.8 \times 10^9$ G. The P_s and $\dot{P}_s$ suggest that PSR J1811−1736 is a mildly recycled pulsar; that is, the spin-up phase via matter accretion from the companion star was too short for the pulsar to reach a spin period of a few milliseconds, typical of fully recycled pulsars. A possible scenario is that the companion was a high-mass star that underwent a supernova explosion, itself turning into a neutron star (Bhattacharya & van den Heuvel 1991). Thus, PSR J1811−1736 might be one of the ∼10 double neutron star (DNS) systems out of the ∼2000 radio pulsars known to date (Manchester et al. 2005). The DNS picture is reinforced by the limits on the companion mass, derived from the mass of the system $M_{tot} = 2.57 \pm 0.10\,M_\odot$ inferred from the measurement of the periastron advance $\dot{\omega} = 0.^\circ0090 \pm 0.^\circ0002$ yr^{-1} and from the mass function. For a pulsar mass $M_P \geq 1.17\,M_\odot$, larger than the minimum value inferred for a radio pulsar (PSR J1518+4904; Janssen et al. 2008), this yields a companion mass of $0.93\,M_\odot \leq M_C \leq 1.5\,M_\odot$ (Corongiu et al. 2007), compatible with that of a neutron star.

A conclusive piece of evidence that PSR J1811−1736 is a DNS would be the detection of its companion as a radio pulsar, as in the

★ E-mail: rm2@mssl.ucl.ac.uk

double pulsar PSR J0737−3039A/B (Lyne et al. 2004). It has, however, escaped detection so far, perhaps because of an unfavourable beaming or because it is no longer in its active radio phase. Alternatively, a conclusive piece of evidence would be the non-detection of the companion in deep optical/infrared (IR) observations. The pulsar companion is not detected in the Digitized Sky Survey (DSS) down to $R \sim 22$ (Mignani 2000) nor in the 2 Micron All Sky Survey (2MASS) down to $K_s \sim 15$, computed at the Lyne et al. (2000) and Corongiu et al. (2007) radio positions, respectively, with the latter limit being quite uncertain owing to the much higher crowding in the pulsar field at IR wavelengths. Such limits would rule out a giant companion but, for the allowed mass range, they would still be compatible with a mid- to late-type main sequence (MS) star, a white dwarf, or a neutron star. No deep optical/near-IR observations of PSR J1811−1736 have been performed so far. As suggested in Mignani (2000), given the substantial interstellar extinction towards the pulsar, near-IR observations are more suited than optical ones to set constraints on the companion star.

Here, we present the results of a new investigation of the PSR J1811−1736 field using IR survey data much deeper than in 2MASS. The observations and results are discussed in Section 2, while the implications for the PSR J1811−1736 companion are discussed in Section 3.

2 INFRARED OBSERVATIONS AND RESULTS

2.1 Observation description

No near-IR observations of PSR J1811−1736 are available in either the ESO[1] or the Gemini[2] Science Data Archives. Thus, we searched for near-IR data of the PSR J1811−1736 field in the image archive of the UK Infrared Deep Sky Survey (UKIDSS) performed with the Wide Field Camera (WFCAM) at the UK Infrared Telescope (UKIRT) at the Mauna Kea Observatory (Hawaii). WFCAM (Casali et al. 2007) is a mosaic detector of four 2048 × 2048 pixel Rockwell devices, with a pixel scale of 0.4 arcsec and covering a field of view of 0.21 square degrees. A general description of the UKIDSS survey is given in Lawrence et al. (2007). The UKIDSS survey covers several regions, with different sky coverages, and sensitivity limits in the *ZYJHK* UKIRT photometric system (Hewett et al. 2006). The field of PSR J1811−1736 is included in the Galactic Plane Survey (GPS; Lucas et al. 2008), which covers about 1800 square degrees in *JHK* down to sensitivity limits that are more than a factor of 10 deeper than 2MASS. Like all the UKIDSS data, the GPS images are processed through a dedicated pipeline (Hambly et al. 2008) developed and operated at the Cambridge Astronomical Survey Unit (CASU), which performs basic reduction steps (dark subtraction, flat-fielding), image de-jittering, stacking, and mosaicking. The pipeline also runs a source detection algorithm and produces source catalogues. Astrometry and photometry calibration are performed using 2MASS stars as a reference (Hodgkin et al. 2009). We searched for the reduced science images of the PSR J1811−1736 field and associated object catalogues through the WFCAM Science Archive (WSA)[3] interface accessible via the Royal Observatory Edinburgh. We queried the most recent UKIDSS Data Release (version 9 Plus) made available on 2011 October 25. The field was observed on 2006 July 18. We downloaded 10 arcmin × 10 arcmin *J*-, *H*- and *K*-band stacks around the pulsar position and the associated multiband object catalogues.

2.2 Pulsar astrometry

For the search for the companion star to PSR J1811−1736, we assumed as a reference its radio timing coordinates. We note that the pulsar radio timing solution presented by Corongiu et al. (2007) is based on data taken in the epoch range MJD = 50842–53624 and does not include the determination of the proper motion of the pulsar, an essential parameter for recomputing its position at a given epoch. For this reason, we re-analysed the data presented in Corongiu et al. (2007) adding the proper motion to the timing model, to obtain a new radio timing position at a reference epoch (MJD = 53624) closest to that of the UKIDSS observation (MJD = 53934). Thus, we obtained $\alpha_{J2000} = 18^{\rm h}11^{\rm m}55\overset{\rm s}{.}0385 \pm 0\overset{\rm s}{.}0029$ and $\delta_{J2000} = -17^\circ36'38\overset{''}{.}45 \pm 0\overset{''}{.}41$ for the position, and $\mu_\alpha \cos(\delta) = 18.3 \pm 9.7$ mas yr^{-1} and $\mu_\delta = -176 \pm 100$ mas yr^{-1} for the proper motion, where all quoted uncertainties are at the 1σ level. The extrapolated timing position at the epoch of the UKIDSS observation (MJD = 53934) is, then, $\alpha_{J2000} = 18^{\rm h}11^{\rm m}55\overset{\rm s}{.}054 \pm 0\overset{\rm s}{.}009$ and $\delta_{J2000} = -17^\circ36'38\overset{''}{.}60 \pm 0\overset{''}{.}42$, with an uncertainty radius of 0.44 arcsec (1σ) that accounts for the position uncertainty owing to the proper motion extrapolation. For comparison, by applying the same timing model as above but without adding the proper motion, we obtain $\alpha_{J2000} = 18^{\rm h}11^{\rm m}55\overset{\rm s}{.}0337 \pm 0\overset{\rm s}{.}0014$ and $\delta_{J2000} = -17^\circ36'37\overset{''}{.}80 \pm 0\overset{''}{.}19$, where the choice of the reference epoch (MJD = 53624) within the range spanned by the timing data is, in this case, arbitrary. Although this position has a nominal uncertainty radius (0.19 arcsec; 1σ) that is smaller than that obtained in the previous case, assuming it as a reference at the epoch of the UKIDSS observations would introduce an unknown systematic uncertainty owing to the neglected pulsar proper motion. For this reason, it is formally less correct than the radio position obtained by fitting the proper motion, despite the latter having a larger uncertainty radius. Nonetheless, in the following section we conservatively consider both positions in our search for the PSR J1811−1736 counterpart. In computing the overall uncertainty on the PSR J1811−1736 position in the UKIDSS images we also accounted for systematics associated with the nominal accuracy on the UKIDSS astrometry calibration (0.05 arcsec rms at low Galactic latitudes; Lawrence et al. 2007), the internal astrometric accuracy of 2MASS ($\lesssim$0.2 arcsec for stars with $15.5 \leq K \leq 13$), and the accuracy on the link of 2MASS to the International Celestial Reference System (0.015 arcsec; Skrutskie et al. 2006).

2.3 Results

The UKIDSS *K*-band image of the PSR J1811−1736 field is shown in Fig. 1(b), compared with the corresponding 2MASS image in (a). For comparison, we plotted the two pulsar positions derived from the radio timing solution, with and without fitting the proper motion. As can be seen, no object is detected within the two 1σ radio position error circles (0.44- and 0.19-arcsec radii, respectively). However, a star ($K = 15.46 \pm 0.02$), unresolved in the 2MASS image but clearly detected in the much higher-resolution UKIDSS one, is detected within the proper motion-corrected 3σ radio error circle (1.32-arcsec radius). Thus, its association with the pulsar cannot be ruled out a priori and needs to be investigated. The star is also detected in the *J* and *H* bands, with magnitudes of $J = 18.61 \pm 0.37$ and $H = 16.65 \pm 0.03$. No other star is detected at, or close

[1] http://archive.eso.org
[2] www.gemini.edu
[3] http://surveys.roe.ac.uk/wsa/

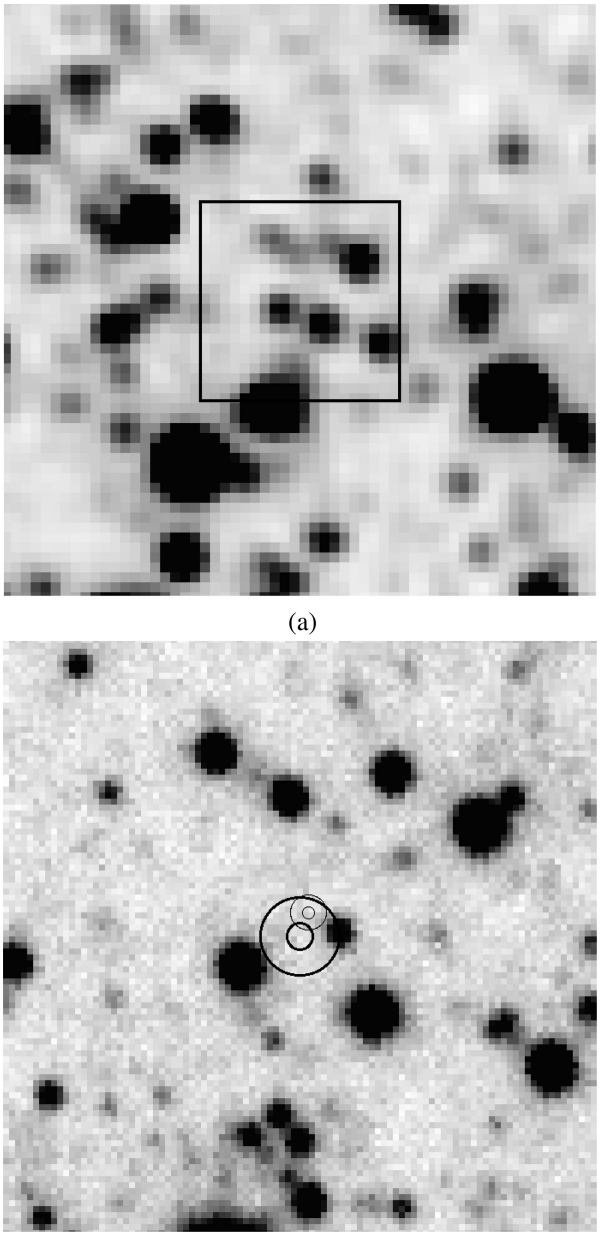

Figure 1. (a) 1 arcmin × 1 arcmin K_s-band image of the PSR J1811−1736 field obtained from 2MASS. The 20 arcsec × 20 arcsec square corresponds to the sky area shown in the bottom panel. (b) K_s-band image zoom of the same field obtained from UKIDSS. North is to the top, east is to the left. The radio positions of PSR J1811−1736 computed with and without fitting its proper motion in the timing model (see Section 2.2) are marked by the two sets of circles, drawn with thick and thin lines, respectively. In both cases, the inner circles correspond to the 1σ (0.44 arcsec; 0.19 arcsec) uncertainty radii, while the outer circles correspond to the 3σ (1.32 arcsec; 0.58 arcsec) ones. The star within the proper motion-corrected 3σ radio error circle (unresolved in the 2MASS image) has magnitudes $J = 18.61 \pm 0.07$, $H = 16.65 \pm 0.03$ and $K_s = 15.46 \pm 0.02$.

to, the computed 3σ radio pulsar positions down to 3σ limiting magnitudes of $J \sim 20.5$, $H \sim 19.4$ and $K \sim 18.6$, as computed from the rms of the sky background (Newberry 1991). Given the high star density along the Galactic plane, however, the match could be the result of a chance coincidence. We computed this probability as $P = 1 - \exp(-\pi\rho r^2)$, where r (∼1.32 arcsec) is the matching radius, assumed equal to the 3σ uncertainty on the proper motion-corrected pulsar radio position, and ρ is the density of stellar objects within an area of 10 arcmin × 10 arcmin around the pulsar. We found that $\rho \sim 0.057$ arcsec^{-2}, which gives $P \sim 0.27$. Such a high chance coincidence probability suggests that the star is probably unrelated to the pulsar, although we need a direct piece of evidence to firmly rule out the association.

3 DISCUSSION

3.1 The interstellar extinction in the pulsar direction

We investigated whether the characteristics of the star detected close to the PSR J1811−1736 position are compatible with its being the companion star. To this end, we tried to determine its spectral type from its colours. Fig. 2 shows the colour–magnitude diagram (CMD) $(H - K)$ versus K and the colour–colour diagram $(K - H)$ versus $(J - K)$ built from the photometry of field stars detected within a 10 arcmin × 10 arcmin area around the pulsar position, as derived from the UKIDSS object catalogue. We have also plotted the location of the star detected close to the PSR J1811−1736 position (Fig. 1b), whose location in both diagrams is consistent with the sequence of field stars. Thus, determining its spectral type from the comparison of its colours and flux with those of field stars is not straightforward. Moreover, the determination of the star's intrinsic colours is affected by the substantial interstellar extinction towards the pulsar, which is located in the Galactic plane ($l = 12.^{\circ}828$; $b = 0.^{\circ}435$). In particular, the CMD is very broadened, suggesting that the field is affected by a high, and probably differential, extinction.

The interstellar extinction towards PSR J1811−1736 is uncertain, and this affects our estimate of the upper limits on the companion star luminosity. A first estimate of the interstellar extinction can be derived from the integrated hydrogen column density along the line of sight to the pulsar. This is $N_{\rm H} = (1.24 - 1.64) \times 10^{22}$, as computed using the HEASARC tool WEBPIMMS[4] according to the Dickey & Lockman (1990) and Kalberla et al. (2005) hydrogen maps. This gives $E(B - V) = 2.2$–2.9, according to the relation of Predhel & Schmitt (1995). However, PSR J1811−1736 is closer than the edge of the Galaxy, at a distance $D = 5.7^{+0.84}_{-0.71}$ kpc, estimated from the radio pulse dispersion measure (DM = 476 ± 5 pc cm^{-3}; Corongiu et al. 2007) and the Galactic free electron density along the line of sight (Cordes & Lazio 2002). This would suggest a lower interstellar extinction. According to the Galactic extinction maps of Hakkila et al. (1997), the pulsar distance and Galactic coordinates imply an interstellar extinction $E(B - V) \sim 1.9$. However, these estimates are only indicative, mainly because of the uncertainties on the extinction maps on smaller angular scales. Unfortunately, the PSR J1811−1736 field has not been observed in the X-ray, so that no independent measurement of the interstellar extinction can be inferred from the hydrogen column density $N_{\rm H}$ directly derived from the fits to the X-ray spectra. In principle, an independent measurement of the $N_{\rm H}$ can be obtained from the DM itself, assuming an average ionization fraction of the interstellar medium (ISM) along the line of sight. In the case of PSR J1811−1736, a DM = 476 ± 5 pc cm^{-3} would correspond to $N_{\rm H} \sim 1.5 \times 10^{22}$ cm^{-2}, for a 10 per cent ionization fraction. This would imply an $E(B - V) \sim 2.7$. However, this method is usually applied to pulsars closer than ∼300 pc (e.g. Pavlov et al. 2009; Tiengo et al. 2011) and is

[4] http://heasarc.nasa.gov/cgi-bin/Tools/w3nh/w3nh.pl

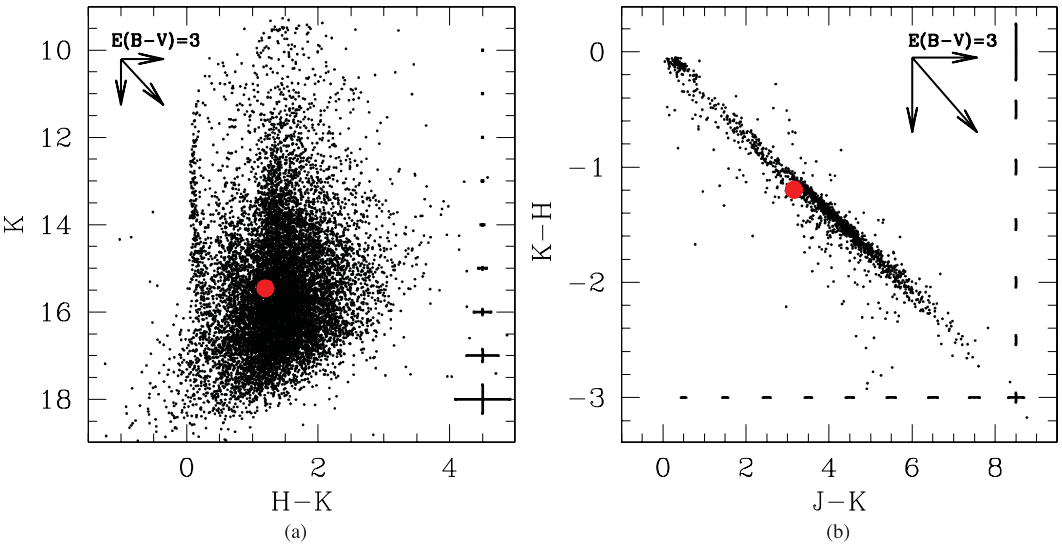

Figure 2. (a) K–$(H-K)$ colour–magnitude diagram of the PSR J1811−1736 field obtained from the UKIDSS photometry of stars detected in a 10 arcmin × 10 arcmin region around the PSR J1811−1736 position. The star detected closest to the pulsar position (see Fig. 1) is marked in red. (b) $(K-H)$ versus $(J-K)$ colour–colour diagram of the same region. The reddening vectors for an $E(B-V)=3$ are shown as a reference. Average photometric errors in the pulsar field, for various magnitude and colour bins, are also plotted in (a) and (b) respectively.

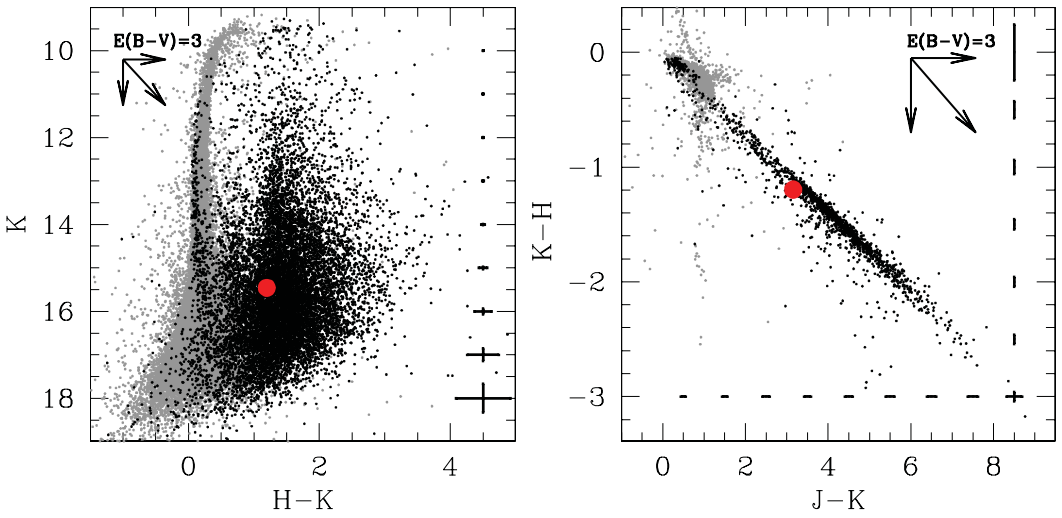

Figure 3. As Fig. 2, but with UKIDSS data for the Baade Window (light grey) overlaid for comparison.

intrinsically affected by a much larger uncertainty for pulsars at larger distances, such as PSR J1811−1736.

We tried to derive an independent estimate on the reddening along the line of sight by comparing the CMDs and colour–colour diagrams of field stars with those in a reference region of very low reddening, such as the Baade Window. As we did for the PSR J1811−1736 field, we extracted from the UKIDSS data the object catalogues relative to a 10 arcmin × 10 arcmin area centred around the Baade Window, for which we assumed the coordinates of the globular cluster NGC 6522: $\alpha_{J2000} = 18^{h}03^{m}34\overset{s}{.}08$ and $\delta_{J2000} = -30^{\circ}02'02\overset{''}{.}3$ (Di Criscienzo et al. 2006). Fig. 3 shows the same diagrams as in Fig. 2 but with the UKIDSS data for the Baade Window region overlaid. From the comparison of the two sets of diagrams, we derived an estimate of the interstellar extinction towards the pulsar. First, we computed the average of the distribution in the colour–colour space for the Baade Window region, applying a 3σ clipping. Second, we did the same for the pulsar field but selecting a region of 50-arcsec radius around the pulsar position not to be affected by the differential extinction in the field. Then, from the difference between the two values we estimated an $E(B-V) = 5.7 \pm 1.9$ for the pulsar field. This value is a factor of 2 larger than the Galactic interstellar extinction inferred from the hydrogen column density maps in the direction of the pulsar. However, we note that the N_{H} value reported above is a weighted average relative to a 1° radius area around the pulsar coordinates, which does not rule out the presence of patches of higher hydrogen column density on angular scales smaller than $0\overset{\circ}{.}4$, which are not resolved by the available maps.

Indeed, it has been found that the interstellar extinction towards the Galactic bulge region is not uniform and shows strong variations, or granularities, on angular scales as small as 1 arcmin (see e.g. Gosling, Blundell & Bandyopadhyay 2006). We used the UKIDSS J-, H- and K_{s}-band images of the PSR J1811−1736 field to measure the granularity of the interstellar extinction in the region, following the method described in Gosling et al. (2006). We considered a region of 500 arcsec × 500 arcsec centred on the PSR J1811−1736

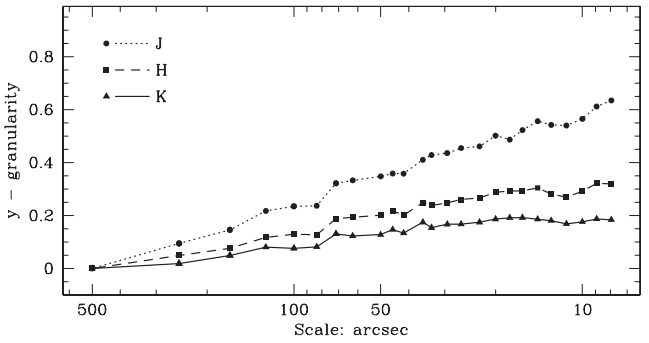

Figure 4. Measure of the granularity on the PSR J1811−1736 field (*y* parameter) computed using the method described in Gosling et al. (2006) as a function of the angular distance from the pulsar. The three curves correspond to the granularity measured in the *J*-, *H*- and K_s-band images (see legend).

position. We divided the region into cells with dimension variable between 8 and 500 arcsec to sample the granularity in the field on different angular scales. For each cell dimension, we calculated the *y* parameter (see equation 1 in Gosling et al. 2006), which gives a quantitative estimate of the granularity of the field and is defined as the variance of the number of stars in all cells normalized to the mean number of stars per cell. We computed the *y* parameter for the *J*-, *H*- and K_s-band images. For the region considered in our analysis, we found that the *y* parameter, and hence the granularity, decreases as a function of wavelength (see Fig. 4), as in the case of one of the test fields used by Gosling et al. (2006). Thus, the high level of granularity in the pulsar field seems to be correlated with a high and variable reddening, explaining the large scatter in the CMD and colour–colour diagram of the field stars (Fig. 2). We note that the measured angular scale of the granularity in the PSR J1811−1736 field (see Fig. 4) is comparable to the 50-arcsec-radius region that we used to estimate the extinction in the direction of the pulsar from the CMD and colour–colour diagram analysis (see previous paragraph). Thus, we are confident that our procedure does not under/overestimate the assumed extinction value along the line of sight to the pulsar.

3.2 The candidate companion star

Under the hypothesis that the star seen close to the PSR J1811−1736 position is its companion, we tried to determine its spectral type assuming the range of reddening values computed above. We considered a range of distances within the computed 1σ uncertainty range on the PSR J1811−1736 distance based on the DM ($D = 4.9$–6.54 kpc), and an age range of 1–13.2 Gyr, consistent with the ages of the stellar populations in the Galactic Centre region (e.g. Zoccali et al. 2003), where the pulsar is located. We also considered different values of the metallicity *Z*. For older populations, we considered both $Z = 0.008$ and $Z = 0.02$, while for the younger populations we considered only $Z = 0.02$. Then, for different values of metallicity, age and distance, we determined the best $E(B-V)$ values in the range $E(B-V) = 3.8$–7.6 that minimize the sum of the projected distances of the star location in the J–$(J-H)$ and K–$(H-K)$ CMDs from the isochrones computed from the stellar models of Marigo et al. (2008) and Girardi et al. (2010). From the best combinations of metallicity, age, distance and reddening, we then derived the corresponding mass (M_C) and radius (R_C) of the candidate companion star to PSR J1811−1736, from comparison with the isochrones. Finally, we combined the computed mass of the candidate companion star with the mass function of the pulsar system (Corongiu et al. 2007) and its total mass ($M_{tot} = 2.57 \pm 0.10\,M_\odot$). In this way, we derived the pulsar mass (M_P) and the orbital inclination angle *i* of the system for each combination of metallicity, age, distance, reddening and mass of the candidate companion star. We filtered out combinations for which it resulted in $\sin i > 1$. We also selected the acceptable combinations for the conditions that the companion mass $0.93\,M_\odot \leq M_C \leq 1.5\,M_\odot$ and the pulsar mass $1.17\,M_\odot \leq M_P \leq 1.6\,M_\odot$, as they result from the PSR J1811−1736 timing analysis (Corongiu et al. 2007), where the lower limit on M_P corresponds to the minimum measured value for the mass of a neutron star (Janssen et al. 2008). The various parameter combinations are summarized in the first eight columns of Tables 1 and 2. These parameters are consistent, for a reddening $E(B-V) = 4.5$–5, with a companion star still on the main sequence (MS) and close to the turn-off or on the lower red giant branch (RGB), with an inferred mass $M_C \sim 1$–$1.3\,M_\odot$ and radius $R_C \sim 4.3$–$5.8\,R_\odot$.

All the combinations of parameters reported in Tables 1 and 2 have been further checked against the lack of eclipses at superior conjunction (orbital phase $\phi = 0.25$) in the radio timing observations. This check is based on the fact that the pulsar cannot be eclipsed at a given orbital phase if the corresponding pulse's time of arrival (ToA) has been determined, as ToA determination strictly requires the detection of the pulse. Hence, we calculated the orbital phases for each ToA presented in Corongiu et al. (2007), and we obtained that the closest available ToAs before and after superior conjunction correspond to an orbital phase $\phi = 0.191366$ and $\phi = 0.277151$, respectively. A particular combination of parameters is acceptable only if, at both orbital phases, the projected distance *d* of the pulsar to the centre of the companion, computed on the plane perpendicular to the line of sight, is larger than the companion radius, namely $d/R_C > 1$. Columns 9 and 10 of Tables 1 and 2 report the values of d/R_C for the two values of the orbital phase computed above, with the possible combinations flagged Yes and No for the cases $d/R_C > 1$ and $d/R_C < 1$, respectively. Our calculation shows that for only 4 out of the 63 possible combinations of selected parameters is the required condition satisfied at both orbital phases. These combinations imply a ∼5-Gyr companion star, with mass $M_C \sim 1.3\,M_\odot$ and radius $R_C \sim 5\,R_\odot$, at a distance of ∼5.5 kpc and with a reddening $E(B-V) \sim 4.9$. This corresponds to a pulsar mass $M_P \sim 1.3\,M_\odot$ and an inclination angle for the system of ∼45°. Thus, according to the constraints on the masses and orbital inclination of the binary system, it is theoretically possible that the star detected at the radio position is, indeed, the companion to the pulsar. In this case, PSR J1811−1736 would not be a DNS.

A ∼5-Gyr MS companion would be compatible with the pulsar spin-down age ($\tau_{SD} = 1.9$ Gyr), but not particularly compatible with the recycling scenario and the pulsar orbital parameters. In principle, the high orbital eccentricity of PSR J1811−1736 ($e = 0.828$) can be seen as the signature of a supernova explosion that changed all binary system parameters. Because PSR J1811−1736 is a recycled pulsar, the orbit must have been circularized during the recycling process (Battacharya & van den Heuvel 1991), and its orbital eccentricity could have been produced by a second supernova explosion, namely that of the companion star. In this case, both the spin period and the orbital eccentricity values of PSR J1811−1736 would be the highest among DNSs and consistent with the correlation between these two parameters observed in such systems Faulkner, Kramer & Lyne (2005) and recovered under the hypothesis of a low-amplitude neutron star kick ($\sigma_v \sim 20$ km s^{-1}) at birth Dewi, Podsiadlowski & Pols (2005).

Table 1. Best parameter combinations for the candidate companion star of PSR J1811−1736 obtained from the comparison between its location in the CMDs and model isochrones. Columns list the star metallicity Z, age (in logarithmic units), distance (D), reddening, mass (M_C) and radius (R_C), the mass of the pulsar (M_P) in solar units, and the system inclination angle (i), obtained from the estimated companion mass, the system mass function, and the total mass. The next two columns list the projected distance (d) of the pulsar to the centre of the companion on the plane perpendicular to the line of sight, normalized to the companion radius R_C for the two values of the orbital phase ϕ when the pulsar is observed closest to the superior conjunction $\phi = 0.25$. The last column flags the acceptable configurations under the condition that $d/R_C > 1$ at both orbital phases (see text).

Z	Log(age) (yr)	D (kpc)	$E(B-V)$	M_C ($M_\odot$)	R_C ($R_\odot$)	M_P ($M_\odot$)	i (deg)	d/R_C $\phi = 0.191366$	d/R_C $\phi = 0.277151$	Flag
0.020	10.12	6.54	4.70	0.97	5.78	1.60	76.11	0.65722	0.37243	No
0.020	10.12	5.70	4.72	0.97	5.02	1.60	76.17	0.75582	0.42761	No
0.020	10.12	4.99	4.76	0.97	4.41	1.60	76.28	0.85852	0.48427	No
0.020	10.10	6.54	4.70	0.99	5.77	1.58	73.56	0.69322	0.41833	No
0.020	10.10	5.70	4.73	0.99	5.03	1.58	73.63	0.79406	0.47843	No
0.020	10.10	4.99	4.76	0.99	4.41	1.58	73.72	0.90401	0.54356	No
0.020	10.08	6.54	4.70	1.00	5.77	1.57	71.36	0.72583	0.45845	No
0.020	10.08	5.70	4.73	1.00	5.03	1.57	71.42	0.83156	0.52463	No
0.020	10.08	4.99	4.77	1.00	4.41	1.57	71.53	0.94628	0.59574	No
0.020	10.06	6.54	4.70	1.01	5.76	1.56	69.47	0.75664	0.49420	No
0.020	10.06	5.70	4.74	1.01	5.04	1.56	69.47	0.86473	0.56480	No
0.020	10.06	4.99	4.77	1.01	4.40	1.56	69.62	0.98739	0.64330	No
0.020	10.04	6.54	4.71	1.02	5.78	1.55	67.74	0.78193	0.52452	No
0.020	10.04	5.70	4.74	1.02	5.03	1.55	67.74	0.89852	0.60273	No
0.020	10.04	4.99	4.78	1.02	4.41	1.55	67.88	1.02185	0.68407	No
0.020	10.02	6.54	4.71	1.03	5.76	1.54	66.11	0.81169	0.55665	No
0.020	10.02	5.70	4.75	1.03	5.03	1.54	66.30	0.92585	0.63339	No
0.020	10.02	4.99	4.78	1.03	4.41	1.54	66.30	1.05601	0.72244	No
0.020	10.00	6.54	4.72	1.05	5.78	1.52	64.72	0.83226	0.58041	No
0.020	10.00	5.70	4.75	1.05	5.03	1.52	64.72	0.95635	0.66695	No
0.020	10.00	4.99	4.79	1.05	4.42	1.52	64.72	1.08834	0.75900	No
0.008	10.00	6.54	4.83	0.97	5.77	1.60	76.04	0.65927	0.37429	No
0.008	10.00	5.70	4.85	0.97	5.02	1.60	76.14	0.75627	0.42821	No
0.008	10.00	4.99	4.88	0.97	4.40	1.60	76.28	0.86047	0.48537	No

We investigated whether the MS companion scenario would indeed be compatible with the pulsar spin and orbital parameters. We compare in Fig. 5 the eccentricity, spin period and orbital period of PSR J1811−1736 with those of binary pulsars with identified companions, whose masses are in the same range as the PSR J1811−1736 companion. We selected our sample from the Australia Telescope National Facility (ATNF) pulsar data base[5] (Manchester et al. 2005). Our sample is summarized in Table 3. In our analysis, we focused on the comparison with recycled binary pulsars only, whose evolutionary path can be compared with that of PSR J1811−1736. As seen, the only known pulsar–MS star system in the selected companion mass range is PSR J1903+0327 (Khargharia et al. 2012). However, this is a fully recycled millisecond-pulsar ($P_s = 2.5$ ms), whereas PSR J1811−1736 is a mildly recycled pulsar with a much longer spin period ($P_s = 104$ ms) and a much shorter orbital period ($P_{orb} = 18.8$ d) than PSR J1903+0327 ($P_{orb} = 95.2$ d). Moreover, the eccentricity of PSR J1811−1736 ($e = 0.828$) is much larger than that of PSR J1903+0327 ($e = 0.436$). Thus, there are no known pulsar–MS star systems in the selected companion mass range with spin and orbital parameters comparable to those of PSR J1811−1736. This might suggest that such systems, if they do exist, are rare, although the very small sample currently available prevents us from drawing firm conclusions. There is one pulsar system, PSR J0514−4002A in the globular cluster NGC 1851 (Freire et al. 2004), with a possible white dwarf (WD) companion (Freire, Ransom & Gupta 2007), that has both orbital period and eccentricity comparable to PSR J1811−1736 (Fig. 5b). However, like PSR J1903+0327, PSR J0514−4002A is a fully recycled pulsar, with a spin period $P_s = 4.99$ ms. Moreover, as PSR J0514−4002A is in a globular cluster, its original companion might have been exchanged through a close encounter with another star in the cluster. Thus, the evolutionary history of this system might not be directly comparable to that of PSR J1811−1736. A firm classification of the PSR J0514−4002A companion would help to evaluate the pulsar–MS star scenario for PSR J1811−1736.

3.3 Constraints on the nature of the companion star

If the companion star of PSR J1811−1736 is undetected in the UKIDSS data, the derived upper limits on its flux can be used to constrain its nature. From the interstellar extinction coefficients of Fitzpatrick (1999), an $E(B-V) = 5.7 \pm 1.9$ would correspond to $A_J \sim 3.3$–6.6, $A_H \sim 2.0$–4.0 and $A_K \sim 1.4$–2.8. From our derived detection limits ($J \sim 20.5$, $H \sim 19.4$ and $K \sim 18.6$), these values imply extinction-corrected fluxes of $J_0 \gtrsim 13.9$, $H_0 \gtrsim 15.4$ and $K_0 \gtrsim 15.8$, where we conservatively assumed the largest values of the interstellar extinction. At the estimated pulsar distance ($D = 5.7^{+0.84}_{-0.71}$ kpc), these values correspond to absolute magnitudes $M_J \gtrsim 6.9$, $M_H \gtrsim 8.4$ and $M_K \gtrsim 8.8$, allowing us to rule out a companion of spectral type earlier than a mid-to-late M-type MS star. Thus, our constraints on the companion star are far more compelling

[5] http://www.atnf.csiro.au/people/pulsar/psrcat/

Table 2. As Table 1 but for ages younger than 10 Gyr.

Z	Log(age) (yr)	D (kpc)	$E(B-V)$	M_C ($M_\odot$)	R_C ($R_\odot$)	M_P ($M_\odot$)	i (deg)	d/R_C $\phi = 0.191366$	d/R_C $\phi = 0.277151$	Flag
0.020	9.98	6.54	4.72	1.06	5.77	1.51	63.27	0.85842	0.60814	No
0.020	9.98	5.70	4.76	1.06	5.04	1.51	63.27	0.98276	0.69623	No
0.020	9.98	4.99	4.78	1.06	4.40	1.51	63.38	1.12323	0.79484	No
0.008	9.98	6.54	4.83	0.99	5.76	1.58	73.50	0.69529	0.42014	No
0.008	9.98	5.70	4.86	0.99	5.03	1.58	73.59	0.79471	0.47925	No
0.008	9.98	4.99	4.88	0.99	4.40	1.58	73.72	0.90607	0.54480	No
0.020	9.96	6.54	4.73	1.07	5.78	1.50	61.93	0.87993	0.63160	No
0.020	9.96	5.70	4.76	1.07	5.03	1.50	61.93	1.01114	0.72577	No
0.020	9.96	4.99	4.79	1.07	4.41	1.50	62.08	1.14991	0.82422	No
0.008	9.96	6.54	4.83	1.00	5.76	1.57	71.30	0.72801	0.46035	No
0.008	9.96	5.70	4.86	1.00	5.02	1.57	71.44	0.83287	0.52525	No
0.008	9.96	4.99	4.88	1.00	4.39	1.57	71.56	0.94999	0.59773	No
0.020	9.94	6.54	4.73	1.08	5.77	1.49	60.71	0.90254	0.65489	No
0.020	9.94	5.70	4.77	1.08	5.04	1.49	60.71	1.03326	0.74975	No
0.020	9.94	4.99	4.80	1.08	4.42	1.49	60.85	1.17504	0.85160	No
0.008	9.94	6.54	4.84	1.01	5.76	1.56	69.47	0.75664	0.49420	No
0.008	9.94	5.70	4.87	1.01	5.01	1.56	69.62	0.86716	0.56498	No
0.008	9.94	4.99	4.89	1.01	4.41	1.56	69.62	0.98515	0.64185	No
0.020	9.92	6.54	4.74	1.10	5.77	1.47	59.57	0.92229	0.67548	No
0.020	9.92	5.70	4.77	1.10	5.03	1.47	59.57	1.05797	0.77486	No
0.020	9.92	4.99	4.80	1.10	4.41	1.47	59.66	1.20467	0.88167	No
0.008	9.92	6.54	4.84	1.02	5.77	1.55	67.74	0.78329	0.52543	No
0.008	9.92	5.70	4.87	1.02	5.03	1.55	67.88	0.89589	0.59975	No
0.008	9.92	4.99	4.89	1.02	4.40	1.55	68.02	1.02117	0.68222	No
0.020	9.90	6.54	4.74	1.11	5.77	1.46	58.40	0.94257	0.69644	No
0.020	9.90	5.70	4.79	1.11	5.06	1.46	58.49	1.07305	0.79233	No
0.020	9.90	4.99	4.81	1.11	4.42	1.46	58.53	1.22751	0.90612	No
0.008	9.90	6.54	4.85	1.03	5.77	1.54	66.17	0.80928	0.55457	No
0.008	9.90	5.70	4.88	1.03	5.03	1.54	66.30	0.92585	0.63339	No
0.008	9.90	4.99	4.89	1.03	4.39	1.54	66.42	1.05819	0.72280	No
0.020	9.80	6.54	4.49	1.18	5.24	1.39	53.51	1.13065	0.86080	No
0.020	9.80	5.70	4.84	1.18	5.12	1.39	53.54	1.15658	0.88040	No
0.020	9.80	4.99	4.75	1.17	4.30	1.40	53.68	1.37393	1.04509	Yes
0.020	9.70	6.54	4.73	1.25	5.67	1.32	48.96	1.12253	0.87220	No
0.020	9.70	5.70	4.80	1.25	5.01	1.32	49.07	1.26832	0.98506	No
0.020	9.70	4.99	4.88	1.25	4.48	1.32	49.17	1.41625	1.09952	Yes
0.020	9.60	6.54	4.84	1.34	5.85	1.23	44.99	1.15094	0.90651	No
0.020	9.60	5.70	4.84	1.34	5.05	1.23	45.09	1.33147	1.04838	Yes
0.020	9.60	4.99	4.90	1.33	4.48	1.24	45.22	1.49824	1.17923	Yes

that those derived by Mignani (2000) on the basis of the DSS data alone. Moreover, those constraints should be now revised upwards as the reddening towards the pulsar measured in this work is at least twice as large as assumed by Mignani (2000) from the Galactic extinction maps (Hakkila et al. 1997). These were, however, the only resources available at the time to determine the reddening in the pulsar direction. 2MASS data of the pulsar field, which could be used to determine the reddening from the CMD technique, as we did with the UKIDSS data, were only released after the Mignani (2000) paper was published. Our new limits are also not deep enough to rule out a WD companion star. As in the previous section, we investigated whether the PSR J1811−1736 spin and orbital parameters would fit those of recycled pulsar–WD systems. As seen from Fig. 5, most recycled pulsar–WD systems have circular orbits and both orbital and spin periods shorter than PSR J1811−1736. There is only one recycled pulsar–WD system, PSR J1750−3703A in the globular cluster NGC 6397 (D'Amico et al. 2001), that has both spin ($P_s = 0.111$ s) and orbital ($P_{orb} = 17.33$ d; $e = 0.712$) parameters close to PSR J1811−1736. Thus, it is possible that PSR J1811−1736 is, indeed, a pulsar–WD system and not a DNS. However, because also PSR J1750−3703A is in a globular cluster, the same caveats as discussed above for PSR J0514−4002A apply in this case. The identification of other pulsar–WD systems with spin and orbital parameters close to those of PSR J1811−1736, but located in the Galactic plane, would help to determine the nature of the PSR J1750−3703A system. We note that the other pulsar–WD system PSR B2303+46 (Dewey et al. 1985; Thorsett et al. 1993; van Kerkwijk & Kulkarni 1999) with orbital parameters ($P_{orb} = 12.33$ d; $e = 0.658$) similar to PSR J1811−1736 (Fig. 5b) is not a recycled pulsar, which means that it is either on a different evolutionary path or at a different evolutionary stage.

4 SUMMARY AND CONCLUSIONS

Using UKIDSS near-IR images, we detected a star, with magnitudes $J = 18.61 \pm 0.37$, $H = 16.65 \pm 0.03$ and $K = 15.46 \pm 0.02$, within the 3σ radio position uncertainty of PSR J1811−1736. In order to determine the spectral type of the star, we estimated the reddening along the line of sight from the comparison of the CMDs of the stellar field with those of the Baade Window, also built

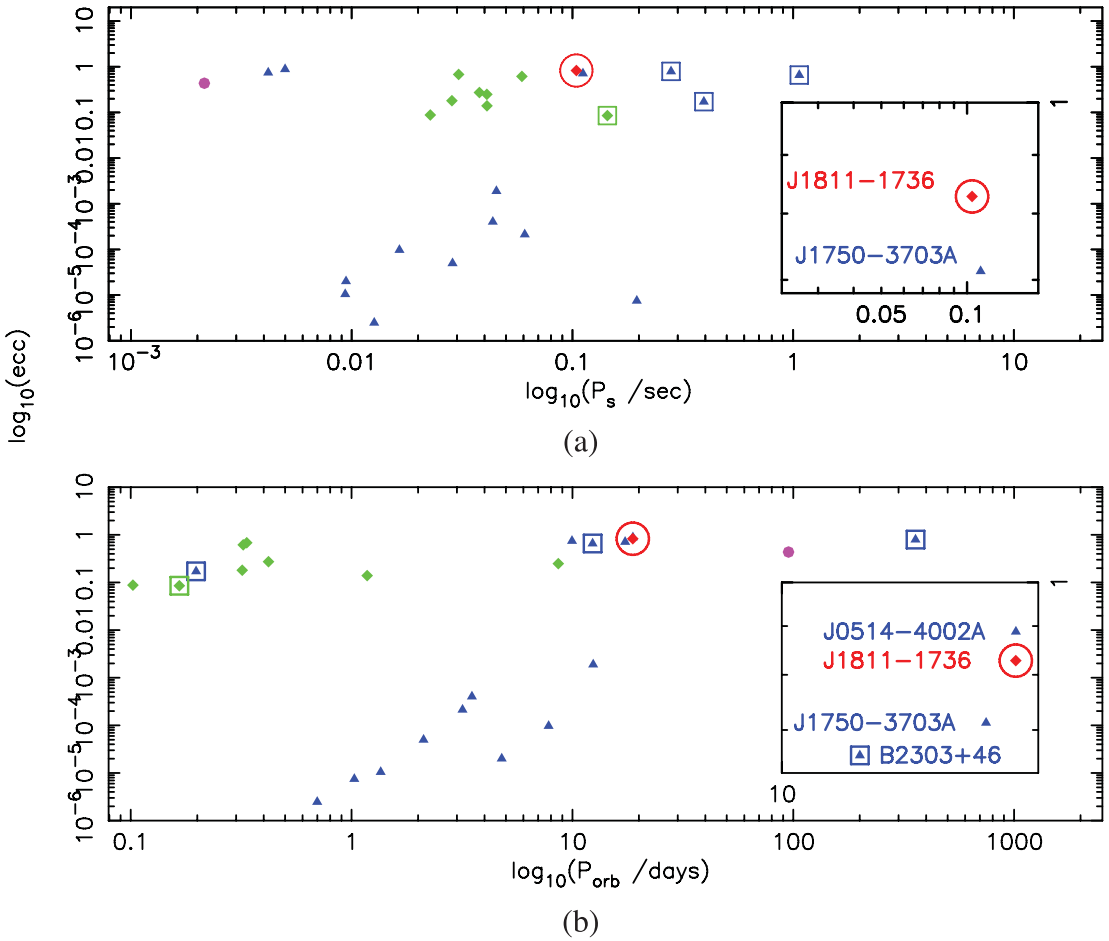

Figure 5. Orbital eccentricity e versus (a) spin P_s and (b) orbital period P_{orb} for the binary pulsars in Table 3. Different symbols and colours correspond to different pulsar systems: DNSs (green diamonds); pulsar–white dwarf (blue triangles); pulsar–MS (magenta filled circle). Squares highlight non-recycled pulsar systems. The location of PSR J1811−1736 is marked by the circled red diamond. The inset shows a zoom of the plots around the location of PSR J1811−1736. Pulsar systems falling closest to PSR J1811−1736 in the e–P_s and e–P_{orb} planes are labelled and colour-coded.

using UKIDSS data. The reddening turns out to be at least twice as large as expected from the Galactic extinction maps. At a pulsar distance of ∼5.5 kpc, and for the estimated reddening of $E(B-V) \sim 4.9$, the star detected near to the radio position could be either a MS star close to the turn-off or a lower RGB star. The inferred mass ($\sim 1.3\,M_\odot$) and radius ($\sim 5\,R_\odot$) of this star could be compatible with the pulsar mass function, the constraints on the pulsar and companion masses, and the lack of radio eclipses near superior conjunction. Thus, it is possible that this star is the pulsar companion, which would reject the DNS scenario for PSR J1811−1736. If this is the case, this might be the first known example of a mildly recycled pulsar–MS star system with companion mass in the ∼0.9–$1.5\,M_\odot$ range, high eccentricity ($e > 0.8$), and spin and orbital periods in the explored range. However, we note that the computed chance coincidence probability of the candidate companion with the proper motion-corrected 3σ radio position is $P \sim 0.27$, which suggests that it might, instead, be an unrelated field star. A conclusive piece of evidence to prove/disprove the association would come from IR spectroscopic observations of the candidate companion star along the orbital phase of the binary system and the comparison of its velocity curve with that predicted by the orbital parameters of PSR J1811−1736. Were the star confirmed to be its companion, this would drive new theoretical studies on the birth and evolution of neutron stars in binary systems, the formation of mildly recycled radio pulsars, and the amplitude of neutron star kicks imparted by supernova explosions. On the other hand, were the star proved to be an unrelated field star, the identification of PSR J1811−1736 as a DNS would remain an open issue. Our near-IR detection limits with UKIDSS only rule out a companion of spectral type earlier than a mid-to-late M-type MS star. Deeper observations with 8-m-class telescopes would enable us to push these limits down by about 4 mag in each band. This would still not be enough to rule out any possible companion other than a neutron star, although a WD would still be compatible with the deepest achievable limits, unless the reddening is much lower than estimated in the current work. However, as shown in Section 3.3, most recycled pulsar–WD systems in the Galactic plane do not fit the spin and orbital parameters of PSR J1811−1736. The detection of PSR J1811−1736 in the X-ray, as for the other DNS PSR J1537+1155 (Durant et al. 2011), would be useful to independently constrain the reddening along the line of sight and place tighter constraints on the absolute luminosity of the companion. Finally, new radio observations of PSR J1811−1736 will be important to derive an updated radio timing position and precisely measure the pulsar proper motion, for which we could only obtain a 2σ measurement using the current radio observation data base. A more precise radio timing position of PSR J1811−1736 will, then, enable us to revisit its association with its candidate companion star.

Table 3. Name, timing (P_s, $\dot{P}_s$, τ_{SD}, B_{surf}) and orbital parameters (P_{orb}, e) for binary pulsars with identified companions and masses in the same range as the PSR J1811−1736 companion. The sample has been selected from the ATNF pulsar data base (Manchester et al. 2005). Pulsar names are sorted according to right ascension. The values of the companion masses M_C are either directly measured or calculated from other parameters (e.g. post-Keplerian parameters). The two extremes of the mass range for M_C are computed assuming an inclination angle $i = 90^\circ$ and $i = 60^\circ$, respectively, and a neutron star mass of $1.35\,M_\odot$. $i = 60^\circ$ is the median orbital inclination, for which there is an equal probability P of having an inclination smaller or larger than 60°; that is, $P(i < 60^\circ) = P(i > 60^\circ) = 0.5$. The last two columns indicate the companion type (WD, NS, MS) and whether the pulsar system is ordinary or recycled.

Name	P_s (s)	$\dot{P}_s$ (s s^{-1})	τ_{SD} (yr)	B_{surf} (G)	P_{orb} (d)	e	M_C ($M_\odot$)	Companion	Ordinary (O)/ Recycled (R)
J0514−4002A	0.004991	1.17×10^{-21}	6.75×10^{10}	7.73×10^{7}	18.7852	8.880×10^{-1}	0.90–1.11	WD	R
B0655+64	0.195671	6.85×10^{-19}	4.52×10^{9}	1.17×10^{10}	1.0287	7.500×10^{-6}	0.66–0.80	WD	R
J0737−3039A	0.022699	1.76×10^{-18}	2.04×10^{8}	6.40×10^{9}	0.1023	8.778×10^{-2}	1.24890	NS	R
J1022+1001	0.016453	4.33×10^{-20}	6.01×10^{9}	8.55×10^{8}	7.8051	9.700×10^{-5}	1.05000	WD	R
J1141−6545	0.393899	4.31×10^{-15}	1.45×10^{6}	1.32×10^{12}	0.1977	1.719×10^{-1}	1.02000	WD	O
J1157−5112	0.043589	1.43×10^{-19}	4.83×10^{9}	2.53×10^{9}	3.5074	4.024×10^{-4}	1.18–1.46	WD	R
J1337−6423	0.009423	1.95×10^{-19}	7.64×10^{8}	1.37×10^{9}	4.7853	2.004×10^{-5}	0.78–0.95	WD	R
J1435−6100	0.009348	2.45×10^{-20}	6.05×10^{9}	4.84×10^{8}	1.3549	1.047×10^{-5}	0.88–1.08	WD	R
J1439−5501	0.028635	1.42×10^{-19}	3.20×10^{9}	2.04×10^{9}	2.1179	4.985×10^{-5}	1.11–1.38	WD	R
J1454−5846	0.045249	8.17×10^{-19}	8.78×10^{8}	6.15×10^{9}	12.4231	1.898×10^{-3}	0.86–1.05	WD	R
J1518+4904	0.040935	2.72×10^{-20}	2.39×10^{10}	1.07×10^{9}	8.6340	2.495×10^{-1}	0.82–0.99	NS	R
J1528−3146	0.060822	2.49×10^{-19}	3.87×10^{9}	3.94×10^{9}	3.1803	2.130×10^{-4}	0.94–1.15	WD	R
B1534+12	0.037904	2.42×10^{-18}	2.48×10^{8}	9.70×10^{9}	0.4207	2.737×10^{-1}	1.35000	NS	R
J1750−3703A	0.111601	5.66×10^{-18}	3.12×10^{8}	2.54×10^{10}	17.3343	7.124×10^{-1}	0.58–0.69	WD	R
J1756−2251	0.028462	1.02×10^{-18}	4.43×10^{8}	5.44×10^{9}	0.3196	1.806×10^{-1}	1.10–1.35	NS	R
J1802−2124	0.012648	7.26×10^{-20}	2.76×10^{9}	9.69×10^{8}	0.6989	2.474×10^{-6}	0.78000	WD	R
J1807−2459B	0.004186	8.23×10^{-20}	8.06×10^{8}	5.94×10^{8}	9.9567	7.470×10^{-1}	1.20640	WD	R
J1811−1736	0.104182	9.01×10^{-19}	1.83×10^{9}	9.80×10^{9}	18.7792	8.280×10^{-1}	0.85–1.04	NS	R
B1820−11	0.279829	1.38×10^{-15}	3.22×10^{6}	6.29×10^{11}	357.7620	7.946×10^{-1}	0.65–0.78	WD	O
J1829+2456	0.041010	5.25×10^{-20}	1.24×10^{10}	1.48×10^{9}	1.1760	1.391×10^{-1}	1.26–1.57	NS	R
J1903+0327	0.002150	1.88×10^{-20}	1.81×10^{9}	2.04×10^{8}	95.1741	4.367×10^{-1}	1.03000	MS	R
J1906+0746	0.144072	2.03×10^{-14}	1.13×10^{5}	1.73×10^{12}	0.1660	8.530×10^{-2}	0.80–0.98	NS	O
B1913+16	0.059030	8.63×10^{-18}	1.08×10^{8}	2.28×10^{10}	0.3230	6.171×10^{-1}	1.3886[a]	NS	R
B2127+11C	0.030529	4.99×10^{-18}	9.70×10^{7}	1.25×10^{10}	0.3353	6.814×10^{-1}	1.354[b]	NS	R
B2303+46	1.066371	5.69×10^{-16}	2.97×10^{7}	7.88×10^{11}	12.3395	6.584×10^{-1}	1.16–1.43	WD	O

[a, b] The values of the companion mass are taken from Weisberg, Nice & Taylor (2010) and Jacoby et al. (2006), respectively, and are not yet implemented in the ANTF pulsar data base

ACKNOWLEDGMENTS

We thank the anonymous members of the ESO Time Allocation Committee, whose suggestions triggered this work, and the anonymous referee for his/her constructive comments on our manuscript.

REFERENCES

Bhattacharya D., van den Heuvel E. P. J., 1991, Phys. Rep., 203, 1
Casali M. et al., 2007, A&A, 467, 777
Cordes J. M., Lazio T. J. W., 2002, preprint (astro-ph/0207156)
Corongiu A., Kramer M., Stappers B. W., Lyne A. G., Jessner A., Possenti A., D'Amico N., Löhmer O., 2007, A&A, 462, 703
D'Amico N., Possenti A., Manchester R. N., Sarkissian J., Lyne A. G., Camilo F., 2001, ApJ, 561, L89
Dewey R. J., Taylor J. H., Weisberg J. M., Stokes G. H., 1985, ApJ, 294, L25
Dewi J. D. M., Podsiadlowski P., Pols O. R., 2005, MNRAS, 363, L71
Di Criscienzo M., Caputo F., Marconi M., Musella I., 2006, MNRAS, 365, 1357
Dickey J. M., Lockman F. J., 1990, ARA&A, 28, 215
Durant M., Kargaltsev O., Volkov I., Pavlov G. G., 2011, ApJ, 741, 65
Faulkner A., Kramer M., Lyne A. G., 2005, ApJ, 618, L119
Fitzpatrick E. L., 1999, PASP, 111, 63
Freire P. C., Gupta Y., Ransom S. M., Ishwara-Chandra C. H., 2004, ApJ, 606, L53
Freire P. C., Ransom S. M., Gupta Y., 2007, ApJ, 662, 1177
Girardi L. et al., 2010, ApJ, 724, 1030
Gosling A. J., Blundell K. M., Bandyopadhyay R., 2006, ApJ, 640, L171
Hakkila J., Myers J. M., Stidham B. J., Hartmann D. H., 1997, AJ, 114, 2043
Hambly N. C. et al., 2008, MNRAS, 384, 637
Hewett P. C., Warren S. J., Leggett S. K., Hodgkin S. T., 2006, MNRAS, 367, 454
Hodgkin S. T., Irwin M. J., Hewett P. C., Warren S. J., 2009, MNRAS, 394, 675
Jacoby B. A., Cameron P. B., Jenet F. A., Anderson S. B., Murty R. N., Kulkarni S. R., 2006, A&AS, 209, 9101
Janssen G. H., Stappers B. W., Kramer M., Nice D. J., Jessner A., Cognard I., Purver M. B., 2008, A&A, 420, 753
Kalberla P. M. W., Burton W. B., Hartmann D., Arnal E. M., Bajaja E., Morras R., Pöppel W. G. L., 2005, A&A, 440, 775
van Kerkwijk M. H., Kulkarni S., 1999, ApJ, 516, L25
Khargharia J., Stocke J. T., Froning C. S., Gopakumar A., Joshi B. C., 2012, ApJ, 744, 183
Lawrence A. et al., 2007, MNRAS, 379, 1599
Lucas P. W. et al., 2008, MNRAS, 391, 136
Lyne A. G. et al., 2000, MNRAS, 312, 698
Lyne A. G. et al., 2004, Sci, 303, 1153
Manchester R. N., Lyne A. G., Camilo F., 2001, MNRAS, 328, 17

Manchester R. N., Hobbs G. B., Teoh A., Hobbs M., 2005, AJ, 129, 1993
Marigo P., Girardi L., Bressan A., Groenewegen M. A. T., Silva L., Granato G. L., 2008, A&A, 482, 883
Mignani R. P., 2000, A&A, 358, L53
Newberry M. V., 1991, PASP, 103, 122
Pavlov G. G., Kargaltsev O., Wong J. A., Garmire G. P., 2009, ApJ, 691, 458
Predhel P., Schmitt J. H. M. M., 1995, A&A, 293, 889
Skrutskie M. F. et al., 2006, AJ, 131, 1163
Thorsett S. E., Arzoumanian Z., McKinnon M. M., Taylor J. H., 1993, ApJ, 405, L29
Tiengo A., Mignani R. P., de Luca A., Esposito P., Pellizzoni A., Mereghetti S., 2011, MNRAS, 412, L73
Weisberg J. M., Nice D. J., Taylor J. H., 2010, ApJ, 722, 1030
Zoccali M. et al., 2003, A&A, 399, 931

This paper has been typeset from a TEX/LATEX file prepared by the author.